

# Overcoming Catastrophic Forgetting with Hard Attention to the Task

Joan Serrà<sup>1</sup> Dídac Surís<sup>1,2</sup> Marius Miron<sup>1,3</sup> Alexandros Karatzoglou<sup>1</sup>

## Abstract

Catastrophic forgetting occurs when a neural network loses the information learned with the first task, after training on a second task. This problem remains a hurdle for general artificial intelligence systems with sequential learning capabilities. In this paper, we propose a task-based hard attention mechanism that preserves previous tasks' information without substantially affecting the current task's learning. An attention mask is learned concurrently to every task through stochastic gradient descent, and previous masks are exploited to constrain such learning. We show that the proposed mechanism is effective for reducing catastrophic forgetting, cutting current rates by 33 to 84%. We also show that it is robust to different hyperparameter choices and that it offers a number of monitoring capabilities. The approach features the possibility to control both the stability and compactness of the learned knowledge, which we believe makes it also attractive for online learning and network compression applications.

## 1. Introduction

With the renewed interest in neural networks, old problems re-emerge, specially if they still had an open solution. That is the case with the so-called catastrophic forgetting or catastrophic interference problem (McCloskey & Cohen, 1989; Ratcliff, 1990). In essence, catastrophic forgetting corresponds to the tendency of a neural network to forget what it learned upon learning from new and/or different information. For instance, when a network is first trained to convergence on one task, and then trained on a second task, it forgets how to perform the first task.

Catastrophic forgetting is an important step in the advancement towards more general artificial intelligence systems (Legg & Hutter, 2007). Such systems should be able

to seamlessly remember different tasks, and to learn them sequentially, following a lifelong learning paradigm (Thrun & Mitchell, 1995). Apart from being more biologically plausible (Clegg et al., 1998), there are many practical situations which require a sequential learning system (cf. Thrun & Mitchell, 1995). For instance, it may be unattainable for a robot to retrain from scratch its underlying model upon encountering a new object/task. After accumulating a large number of objects/tasks and their corresponding information, performing concurrent/multitask learning at scale may be too costly.

Storing a certain amount of previous information and using it to retrain the model was among the earliest attempts to overcome catastrophic forgetting; a strategy named “rehearsal” (Robins, 1995). The use of memory modules to alleviate catastrophic forgetting has been a subject of research until today (Rebuffi et al., 2017; Lopez-Paz & Ranzato, 2017). However, due to efficiency and capacity constraints, memory-free approaches were also introduced, starting with what was termed as “pseudo-rehearsal” (Robins, 1995). This approach has found some success in transfer learning situations where one needs to maintain a certain accuracy on the source task after learning the target task (Jung et al., 2016; Li & Hoiem, 2017). Within the pseudo-rehearsal category, we could also consider recent approaches that substitute the memory module by a generative network (Venkatesan et al., 2017; Shin et al., 2017; Nguyen et al., 2017). Besides the difficulty of training a generative network for a sequence of tasks or certain types of data, both rehearsal and pseudo-rehearsal approaches imply some form of concurrent learning, that is, having to re-process ‘old’ instances for learning a new task.

The other popular strategy to overcome catastrophic forgetting is to reduce representational overlap (French, 1991). This can be done at the output, intermediate, and also input levels (Gutsein & Stump, 2015; He & Jaeger, 2017). A clean way of doing that in a soft manner is through so-called “structural regularization” (Zenke et al., 2017), either present in the loss function (Kirkpatrick et al., 2017; Zenke et al., 2017) or at a separate merging step (Lee et al., 2017). With these strategies, one seeks to prevent major changes in the weights that were important for previous tasks. Dedicating specific sub-parts of the network for each task is another way of reducing representational overlap (Rusu et al., 2016;

<sup>1</sup>Telefónica Research, Barcelona, Spain <sup>2</sup>Universitat Politècnica de Catalunya, Barcelona, Spain <sup>3</sup>Universitat Pompeu Fabra, Barcelona, Spain. Correspondence to: Joan Serrà <joan.serra@telefonica.com>.

Fernando et al., 2017; Yoon et al., 2017). The main trade-off in representational overlap is to effectively distribute the capacity of the network across tasks while maintaining important weights and reusing previous knowledge.

In this paper, we propose a task-based hard attention mechanism that allows to maintain previous tasks' information without substantially affecting the learning of a new task. In essence, we learn almost-binary attention vectors through gated task embeddings using minibatch stochastic gradient descent (SGD), and we do it together with the learning of the current task. Previous tasks' attention vectors are then used to define a mask and constrain the update of the network weights. Since such mask is almost binary, a portion of the weights remains static while the rest adapt to the new task. We call our approach hard attention to the task (HAT). We evaluate the performance of HAT in the context of image classification, using what we believe is a high-standard evaluation protocol. We use 8 common and publicly-available data sets representing different tasks, and present them in random sequential order. We compare against a dozen of recent and competitive approaches, showing favorable results in 4 different experimental settings. We also demonstrate a certain robustness with respect to hyperparameters and showcase a number of monitoring capabilities. The code used for the experiments reported in this paper is publicly-available<sup>1</sup>.

## 2. Putting Hard Attention to the Task

### 2.1. Motivation

The primary observation that drives the proposed approach is that the task definition or, more pragmatically, its identifier, is crucial for the operation of the network. Consider the task of differentiating between birds and dogs. When training the network to do so, it may learn all kind of features that are discriminative for that task. Next, when the second task is to differentiate between brown and black animals using the same data (assuming it only contained birds and dogs that were either brown or black), the network may learn a different set of features with not much overlap with the ones of the first task. Clearly, if training data is the same in both tasks, the difference is the task description or identifier. Our intention is to learn to use the task identifier to condition every layer, and to later exploit this learned conditioning to prevent forgetting previous tasks.

### 2.2. General Architecture

To condition to the current task  $t$ , we employ a layer-wise attention mechanism (Fig. 1, top). Given the output of layer  $l$ ,  $\mathbf{h}_l$ , we component-wise multiply  $\mathbf{h}'_l = \mathbf{a}_l^t \odot \mathbf{h}_l$ . However,

<sup>1</sup>Code will be available soon, after cleaning and commenting, and earlier than an eventual conference acceptance.

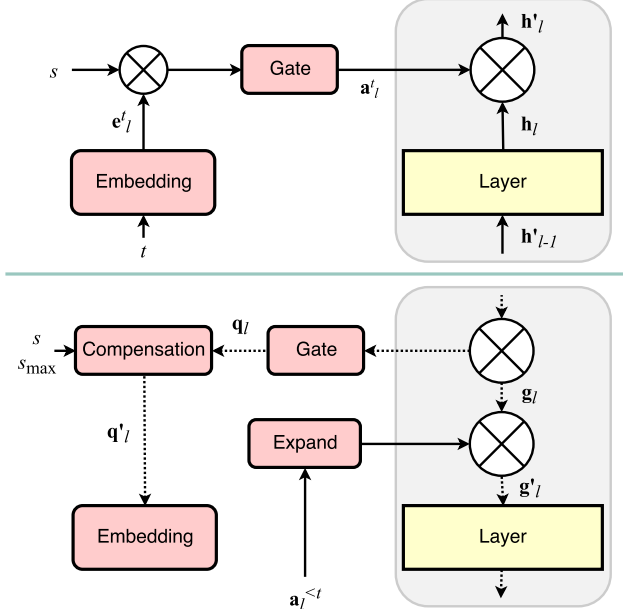


Figure 1. Schematic diagram of the proposed approach: forward (top) and backward (bottom) passes.

an important difference with common attention mechanisms is that, instead of forming a probability distribution,  $\mathbf{a}_l^t$  is a gated version of a task embedding  $\mathbf{e}_l^t$ . More specifically,

$$\mathbf{a}_l^t = \sigma(s\mathbf{e}_l^t), \quad (1)$$

where  $\sigma(x) \in [0, 1]$  is a gate function and  $s$  is a positive scaling parameter. We use a sigmoid gate in our experiments, but we note that other gating mechanisms could be used. All layers  $l = 1, \dots, L-1$  operate equally except the last one, where  $\mathbf{a}_L^t$  is binary hard-coded. The operation of layer  $L$  is equivalent to a multi-head output (Bakker & Heskes, 2003), which has been exploited in the context of catastrophic forgetting by a number of works (for example Rusu et al., 2016; Li & Hoiem, 2017; Nguyen et al., 2017).

The rationale behind the gating mechanism in Eq. 1 is to form a hard attention mask, with possible binary output, that can activate or deactivate a given unit<sup>2</sup> in  $\mathbf{h}_l^t$ . This way, like PathNet (Fernando et al., 2017), we dynamically create and destroy paths across layers that can be later preserved when learning a new task. However, unlike PathNet, the paths in HAT are not based on modules, but on single units. Therefore, we do not need to pre-assign a module size nor to set a maximum number of modules per task. Given some network architecture, HAT learns individual unit paths and automatically dimensions their total number to the task at hand. Furthermore, instead of learning them in a separate stage using genetic algorithms, HAT learns them together

<sup>2</sup>In the remaining of the paper, we will talk about 'units' to refer to both linear units (or fully-connected neurons) and convolutional filters. HAT can be equally used with both.

with the rest of the network, using vanilla SGD.

### 2.3. Network Training

To preserve the information learned in previous tasks upon learning a new task, we condition the network weights' gradients according to the cumulative attention from all the previous tasks. To obtain a cumulative attention vector, after learning task  $t$  and obtaining  $\mathbf{a}_l^t$ , we compute

$$\mathbf{a}_l^{\leq t} = \max(\mathbf{a}_l^t, \mathbf{a}_l^{t-1}),$$

using component-wise maximum and the all-zero vector for  $\mathbf{a}_l^0$ . By using this recursion, we preserve the attention values for units that were important for previous tasks, allowing them to condition the training of future tasks.

To condition the training of task  $t + 1$ , we modify the gradients  $g_{l,ij}$  at layer  $l$  using the reverse of the minimum of the attention mask at the current and previous layers:

$$g'_{l,ij} = \left[1 - \min\left(a_{l,i}^{\leq t}, a_{l-1,j}^{\leq t}\right)\right] g_{l,ij}, \quad (2)$$

where the indices  $i$  and  $j$  correspond to the output (layer  $l$ ) and input (layer  $l - 1$ ) units, respectively. In other words, we expand the vectors  $\mathbf{a}_l^{\leq t}$  and  $\mathbf{a}_{l-1}^{\leq t}$  to match the dimensions of the gradient tensor of the corresponding layer and then perform component-wise operations (Fig. 1, bottom). In the case of the input layer,  $l = 1$ , we do not compute any attention over the input data. However, in the case such input data consisted of separate or independent features, one could also consider them as an output of a certain layer and apply the same methodology.

Note that, with Eq. 2, we are creating masks to constrain the gradients and prevent large updates in the weights that were important for previous tasks. This is similar to the approach of PackNet (Mallya & Lazebnik, 2017), which was introduced concurrently to the development of HAT. In PackNet, after an heuristic selection and retraining, a binary mask is found and later applied to freeze the corresponding network weights. In this regard, HAT differs from PackNet in three important aspects. Firstly, our mask is learned, instead of heuristically or rule-driven. Therefore, HAT does not need to pre-assign compression ratios nor to determine parameter importance through a post-training step. It can thus automatically adapt to different data and tasks. Secondly, the mask used by HAT is not necessarily binary, allowing intermediate values between 0 and 1. This can be useful if we want to reuse weights for learning other tasks, at the expense of some forgetting, or we want to work in a more online mode, forgetting the oldest tasks to remember new ones (this could be achieved by, for instance, setting  $a_{l,ij}$  at a maximum of 0.99 or 0.999 instead of 1). Thirdly, our mask is unit-based, with weight-based masks automatically derived from those (Eq. 2). Therefore, instead of having a mask as large as

the entire network, HAT stores and maintains a much more lightweight structure (essentially, the embeddings, with as many weights as units in the network).

### 2.4. Hard Attention Training

To obtain a totally binary attention vector  $\mathbf{a}_l^t$ , one could use a unit step function as gate. However, if we want to train the embeddings  $\mathbf{e}_l^t$  with SGD (Fig. 1), we need a differentiable function. To construct a pseudo-step function that allows the gradient to flow, we use a sigmoid with a positive scaling parameter  $s$  (Eq. 1). This scaling is introduced to control the polarization, or 'hardness', of the pseudo-step function and the resulting output  $\mathbf{a}_l^t$ . Our strategy is to anneal  $s$  during training, inducing a gradient flow, and set  $s = s_{\max}$  during testing, using  $s_{\max} \gg 1$  such that Eq. 1 approximates a unit step function. Notice that when  $s \rightarrow \infty$ , we get  $a_{l,i}^t \rightarrow \{0, 1\}$ . Notice furthermore that, when  $s \rightarrow 0$ , we get  $a_{l,i}^t \rightarrow 1/2$ . We will use the latter to start a training epoch with all network units being active, and progressively polarize them within the epoch.

During a training epoch, we incrementally linearly anneal the value of  $s$  by

$$s = \left(s_{\max} - \frac{1}{s_{\max}}\right) \frac{b-1}{B-1} + \frac{1}{s_{\max}}, \quad (3)$$

where  $b = 1, \dots, B$  is the batch index and  $B$  is the total number of batches in an epoch. The hyperparameter  $s_{\max} \geq 1$  controls the stability of the learned tasks or, in other words the plasticity of the network's units. For instance, if  $s_{\max}$  is close to 1, the gating mechanism operates like a regular sigmoid function, without particularly enforcing the binarization of  $\mathbf{a}_l^t$ . This provides plasticity to the units, with the model being able to forget previous tasks at the backpropagation stage (Sec. 2.3). If, alternatively,  $s_{\max}$  is a larger number (usually in the range of 100 in our experiments), the gating mechanism starts operating like a unit step function, with  $a_{l,i}^t \rightarrow \{0, 1\}$ . This provides stability with regard to previously learned tasks, preventing changes in the corresponding weights at the backpropagation stage.

### 2.5. Embedding Gradient Compensation

In preliminary analysis, we empirically observed that embeddings  $\mathbf{e}_l^t$  were not changing much, and that the magnitude of the gradient was weak on those weights. After some investigation, we realized that the major part of the problem was due to the introduced annealing scheme (Eq. 3). To illustrate the effect of the annealing scheme on the gradient updates of  $\mathbf{e}_l^t$ , consider a uniformly distributed embedding  $e_{l,i}^t$  across the active range of a standard sigmoid,  $e_{l,i}^t \in [-6, 6]$ . If we do not perform any annealing and set  $s = 1$ , we obtain a cumulative gradient after one epoch that has a bell-like shape and spans the whole sigmoid range (Fig. 2). Con-

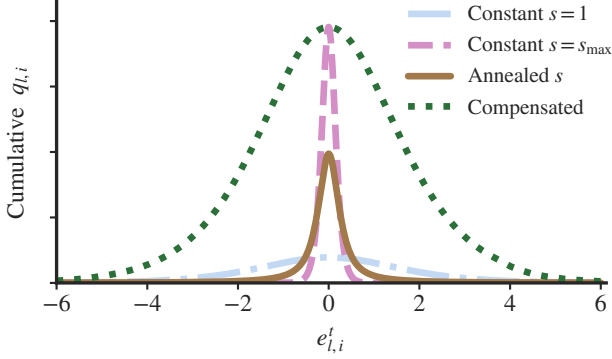


Figure 2. Illustration of the effect that annealing  $s$  has on the gradient updates  $q$  of  $\mathbf{e}_l^t$ .

trastingly, if we set  $s = s_{\max}$ , we obtain a much larger cumulative gradient magnitude, but in a much lower range ( $e_{l,i}^t \in [-1, 1]$  in Fig. 2). The annealed version of  $s$  yields a distribution in-between, with a lower range than  $s = 1$  and a lower magnitude than  $s = s_{\max}$ . Nonetheless, our ideal situation would be to have a wider range, ideally spanning the range of  $s = 1$ , and a larger cumulative magnitude, ideally proportional to the one in the active region when  $s = s_{\max}$ . To achieve that, we apply a gradient compensation before performing the updates on  $\mathbf{e}_l^t$ .

In essence, the idea of the embedding gradient compensation is to remove the effects of the annealed sigmoid and artificially impose the desired range and magnitude motivated in the previous paragraph. To do so, we divide the gradient  $q_{l,i}$  by the derivative of the annealed sigmoid, and multiply by the desired compensation, that is,

$$q'_{l,i} = \frac{s_{\max} \sigma(e_{l,i}^t) [1 - \sigma(e_{l,i}^t)]}{s \sigma(se_{l,i}^t) [1 - \sigma(se_{l,i}^t)]} q_{l,i},$$

which, after operating, yields

$$q'_{l,i} = \frac{s_{\max} [\cosh(se_{l,i}^t) + 1]}{s [\cosh(e_{l,i}^t) + 1]} q_{l,i}.$$

For numerical stability, we clamp  $|se_{l,i}^t| \leq 50$  and constrain  $e_{l,i}^t$  to remain within the active range of the standard sigmoid,  $e_{l,i}^t \in [-6, 6]$ . In any case, however,  $q_{l,i} \rightarrow 0$  when we hit those limits. That is, we are in the constant range of the step function. Notice also that the minimum  $s$  is never equal to 0 (Eq. 3).

## 2.6. Promoting Low Capacity Usage

It is important to realize that the hard attention values  $a_{l,i}^t$  that are ‘active’, that is,  $a_{l,i}^t \rightarrow 1$ , directly determine the units that will be dedicated to (or spend on) task  $t$ . Therefore,

in order to have some model capacity left for future tasks, we want to promote sparsity on the set of attention vectors  $\mathbf{A}^t = \{\mathbf{a}_1^t, \dots, \mathbf{a}_{L-1}^t\}$ . To do so, we add a regularization term to the loss function  $\mathcal{L}$ :

$$\mathcal{L}'(\mathbf{y}, \hat{\mathbf{y}}, \mathbf{A}^t) = \mathcal{L}(\mathbf{y}, \hat{\mathbf{y}}) + cR(\mathbf{A}^t),$$

where  $c$  is the regularization constant,

$$R(\mathbf{A}^t) = \frac{\sum_{l=1}^{L-1} \sum_{i=1}^{N_l} a_{l,i}^t}{\sum_{l=1}^{L-1} N_l}$$

is a normalized L1 regularization over the attention values  $a_{l,i}^t$ , and  $N_l$  corresponds to the number of units in layer  $l$ . The hyperparameter  $c$  controls the capacity spent on each task. In a sense, it can be thought of as a compressibility constant, affecting the compactness of the learned models: the higher the  $c$ , the lower the number of active attention values  $a_{l,i}^t$ , and the more sparse the resultant network is. We set  $c$  globally for all tasks and let HAT learn the best compression for each individual task (Sec. 4.4).

The usage of L1 regularization to promote network sparseness in the context of catastrophic forgetting has also been introduced by Yoon et al. (2017) in the dynamically expandable networks (DEN) approach, which was made public during the development of HAT. In DEN, L1 regularization is used together with a considerable set of heuristics, L2-transfer, and a measure of ‘semantic drift’, among others, and is applied to all network weights in the so-called ‘selective retraining’ phase. In HAT, the L1 regularization is an integral part of the single training phase of the approach, and is applied to the hard attention mask of every task, which is orders of magnitude smaller than the total number of network weights.

## 3. Related Works

We now further compare the proposed approach with the conceptually closest related works, some of which appeared concurrently to the development of HAT. A more general overview of related work has been done in Sec. 1. A qualitative comparison of the most related strategies has been done along Sec. 2. A quantitative comparison with these and other works is done in Sec. 4 and Appendix C.

Both elastic weight consolidation (EWC; Kirkpatrick et al., 2017) and synaptic intelligence (SI; Zenke et al., 2017) approaches add a soft structural regularization term to the loss function in order to discourage changes to weights that are important for previous tasks. HAT uses a hard structural regularization, and does it both at the loss function and gradient updates. EWC and SI measure weights’ importance after network training using different formulation, while HAT learns weights importance concurrently to network training using SGD.

Progressive neural networks (PNNs; [Rusu et al., 2016](#)) distribute the network weights in a column-wise fashion, pre-assigning one column per task. They then employ so-called adapters to reuse knowledge from previous columns/tasks, leading to a progressive increase of the number of weights assigned to every new task. Instead of blindly pre-assigning column widths for future tasks, HAT learns such ‘widths’, together with the network weights, adapting them to the difficulty of the task. PathNet ([Fernando et al., 2017](#)) also pre-assigns some amount of network capacity per task but, in contrast to PNNs, it avoids network columns and adapters. Instead, it uses an evolutionary approach to learn paths between a constant number of so-called modules (layer subsets) that interconnect between themselves, using several hyperparameters. HAT does not maintain a population of solutions nor does it rely on a constant set of modules. The number of hyperparameters is also much lower (only two).

Together with PNNs and PathNet, PackNet ([Mallya & Lazebnik, 2017](#)) also employs a binary mask to constrain the network weights. However, such constrain is not based on columns nor layer modules, but on network weights. Therefore, it allows for a potentially better use of the network’s capacity. Nonetheless, PackNet is based on heuristic weight pruning, with pre-assigned pruning ratios. HAT also focuses on network weights, but uses unit-based masks to constrain those, which results in a much more lightweight structure. HAT also avoids any absolute and/or pre-assigned pruning ratio, although it uses the compressibility parameter  $c$  to influence the compactness of the learned models. Another difference between HAT and the previous three approaches is that it does not use purely binary masks. Instead, the stability parameter  $s_{\max}$  controls the degree of binarization.

Dynamically expandable networks (DEN; [Yoon et al., 2017](#)) also assign network capacity depending on the task at hand. However, they do so in a separate stage called “selective retraining”. A complex mixture of heuristics and hyperparameters is used to identify “drifting” units, which are duplicated and retrained in another stage. L1 regularization and L2-transfer are also used to condition learning, together with the corresponding regularization constants and an additional set of thresholds. HAT strives for simplicity, restricting the number of hyperparameters to two that have a straightforward conceptual interpretation. In addition, the HAT mechanism is a lightweight structure that can be plugged in without the need of introducing important changes to the existing network.

## 4. Experiments

**Setups** — Common setups to evaluate catastrophic forgetting in a classification context are based on permutations of the MNIST data ([Srivastava et al., 2013](#)), label splits of the MNIST data ([Lee et al., 2017](#)), incrementally learn-

ing classes of the CIFAR data sets ([Lopez-Paz & Ranzato, 2017](#)), or two-task transfer learning setups where accuracy is measured on both source and target tasks ([Li & Hoiem, 2017](#)). Nonetheless, there are some limitations with these setups. Firstly, performing permutations of the MNIST data set has been suggested to favor certain approaches and yield misleading results<sup>3</sup> in the context of catastrophic forgetting ([Lee et al., 2017](#)). Secondly, using only the MNIST data may not be very representative of modern computer vision tasks, nor particularly challenging ([Xiao et al., 2017](#)). Thirdly, incrementally adding classes or groups of classes implies the assumption that all data comes from the same joint distribution, which is unrealistic for a real-world setting. Finally, evaluating catastrophic forgetting with only two tasks biases the conclusions towards transfer learning results, and prevents the analysis of truly sequential learning with more than two tasks. In this paper, we consider the aforementioned MNIST and CIFAR setups (Sec. 4.2). However, we primarily evaluate on a sequence of multiple tasks formed by different image classification data sets (Sec. 4.1).

We consider a number of tasks and uniformly randomize their order. After training task  $t$ , we compute the accuracies on all testing sets of tasks  $\tau \leq t$ . We repeat 10 times this sequential training/testing procedure with 10 different seed numbers, which are also used in the rest of randomizations/initializations (see below). To compare between different task accuracies, and in order to obtain a general measurement of the amount of forgetting, we introduce the forgetting ratio

$$\rho^{\tau \leq t} = \frac{A^{\tau \leq t} - A_R^\tau}{A_J^{\tau \leq t} - A_R^\tau} - 1, \quad (4)$$

where  $A^{\tau \leq t}$  is the accuracy measured on task  $\tau$  after sequentially learning task  $t$ ,  $A_R^\tau$  is the accuracy of a random, frequency-based classifier solely trained on task  $\tau$ , and  $A_J^{\tau \leq t}$  is the accuracy measured on task  $\tau$  after jointly learning all  $t$  tasks in a multitask fashion. Note that  $\rho \approx -1$  and  $\rho \approx 0$  correspond to performances close to the ones of the random and multitask classifiers, respectively. To report a single number after learning  $t$  tasks, we take the average

$$\rho^{\leq t} = \frac{1}{t} \sum_{\tau=1}^t \rho^{\tau \leq t}.$$

**Data** — We consider 8 common image classification data sets and adapt them, if necessary, to an input size of  $32 \times 32 \times 3$  pixels by resizing, zero-padding, or replicating values. The number of classes goes from 10 to 100, training

<sup>3</sup>Essentially, the MNIST data contains many values close to 0 that allow for an easier identification of the important units or weights which, if permuted, can then be easily frozen without overlapping with the ones of the other tasks (cf. [Lee et al., 2017](#)).

set sizes from 16,853 to 73,257, and test set sizes from 1,873 to 26,032. For each task, we randomly split 15% of the training set and keep it for validation purposes. The considered data sets are: CIFAR10 and CIFAR100 (Krizhevsky, 2009), FaceScrub (Ng & Winkler, 2014), FashionMNIST (Xiao et al., 2017), NotMNIST (Bulatov, 2011), MNIST (Le-Cun et al., 1998), SVHN (Netzer et al., 2011), and TrafficSigns (Stallkamp et al., 2011). For further details we refer to Appendix A.

**Baselines** — We consider 2 reference approaches plus 9 recent and competitive ones: standard SGD with dropout (Goodfellow et al., 2014), SGD freezing all layers except the last one (SGD-F), EWC, incremental moment matching (IMM-Mean and IMM-Mode; Lee et al., 2017), learning without forgetting (LWF; Li & Hoiem, 2017), less-forgetting learning (LFL; Jung et al., 2016), PathNet, and PNNs. To find the best parameter combination for each approach, we perform a grid search using a task sequence determined by a single seed. To compute the forgetting ratio  $\rho$  (Eq. 4), we also run the aforementioned random and multitask classifiers.

**Network** — Unless stated otherwise, we use an AlexNet-like architecture (Krizhevsky et al., 2012) with 3 convolutional layers of 64, 128, and 256 filters with  $4 \times 4$ ,  $3 \times 3$ , and  $2 \times 2$  kernel sizes, respectively, and two fully-connected layers of 2048 units each. We use rectified linear units as activations and  $2 \times 2$  max-pooling after the convolutional layers. We also use a dropout of 0.2 for the first two layers and of 0.5 for the rest. A fully-connected layer with a softmax output is used as a final layer, together with categorical cross entropy loss. All layers are randomly initialized with Xavier uniform initialization (Glorot & Bengio, 2010) except the embedding layers, for which we use a Gaussian distribution  $\mathcal{N}(0, 1)$ . We adapt the same base architecture to all baseline approaches and match their number of parameters to 7.1 M.

**Training** — We train all models with plain SGD, using a learning rate of 0.05, and decaying it by a factor of 3 if there is no improvement on the validation loss for 5 consecutive epochs. All methods use the same train/validation/test split for a given seed number. We stop training when we reach a learning rate lower than  $10^{-4}$  or we have iterated over 200 epochs (we made sure that all considered approaches reached a stable solution before 200 epochs).

#### 4.1. Results

We first look at the average forgetting ratio  $\rho^{\leq t}$  after learning task  $t$  (Fig. 3). A first thing to note is that not all the considered baselines perform better than the reference approaches SGD and SGD-F. That is the case of LWF and LFL. For LWF, we observe it is competitive in the two-task setting for which it was designed,  $t = 2$ . However, its performance rapidly degrades for  $t > 2$ , indicating that the approach has

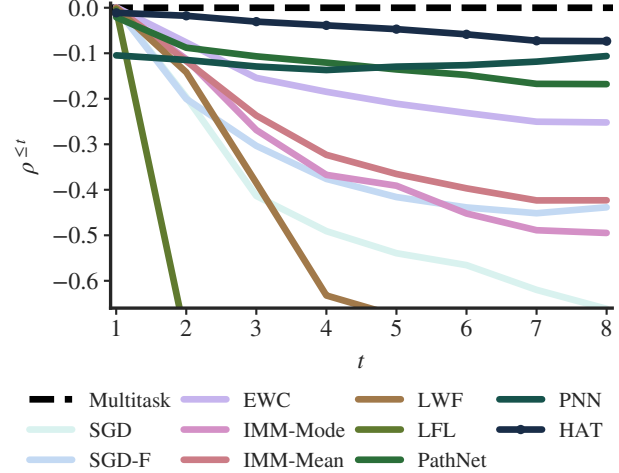


Figure 3. Average forgetting ratio  $\rho^{\leq t}$  for the considered approaches (10 runs).

difficulties in extending beyond a transfer learning setting. For LFL, we found it was extremely sensitive to the configuration of its hyperparameter, to the point that what was a good value for one seed, turned out to be a bad choice for another seed. Hence the poor average performance for 10 seeds. Another thing to note is that the IMM approaches perform similarly or slightly better than the reference ones. We believe this is due to both the different nature of the tasks’ data and the consideration of more than two tasks, which difficults the choice of the mixing hyperparameter.

The best performing baselines are EWC, PathNet, and PNN. PathNet and PNN present contrasting behaviors. Both, by construction, never forget. Therefore, the important difference is in their learning capability. PathNet starts by correctly learning the first two tasks and progressively presenting difficulties to do so for  $t > 2$ . Contrastingly, PNNs have more difficulty in the first tasks while becoming better in the last ones. These contrasting behaviors are due to the way the two approaches allocate the network capacity. In the absence of any other information about the tasks, they cannot do it dynamically, and therefore need to pre-assign a number of network weights per task. In the case we had more than 8 tasks and the same total network capacity, this pre-assignment would increasingly harm the performance of those baselines, lowering the corresponding curves in Fig. 3.

We now move to the HAT results. First of all, we observe that HAT consistently performs better than all considered baselines for all  $t > 1$  (Fig. 3). For the case of  $t = 2$ , it obtains an average forgetting ratio  $\rho^{\leq 2} = -0.03$ , while the best baseline is EWC with  $\rho^{\leq 2} = -0.08$  (Table 1). For the case of  $t = 8$ , it obtains  $\rho^{\leq 8} = -0.07$ , while the best baseline is PNN with  $\rho^{\leq 8} = -0.11$ . This implies a reduction in forgetting of 62 and 36% for  $t = 2$  and  $t = 8$ , respectively.

Table 1. Average forgetting ratio after the second ( $\rho^{\leq 2}$ ) and the last ( $\rho^{\leq 8}$ ) task for the considered approaches (10 runs, standard deviation into parenthesis).

APPROACH	$\rho^{\leq 2}$	$\rho^{\leq 8}$
LFL	-0.73 (0.29)	-0.92 (0.08)
LWF	-0.14 (0.13)	-0.80 (0.06)
SGD	-0.20 (0.08)	-0.66 (0.03)
IMM-MODE	-0.11 (0.08)	-0.49 (0.05)
SGD-F	-0.20 (0.15)	-0.44 (0.06)
IMM-MEAN	-0.12 (0.10)	-0.42 (0.04)
EWC	-0.08 (0.06)	-0.25 (0.03)
PATHNET	-0.09 (0.16)	-0.17 (0.23)
PNN	-0.11 (0.10)	-0.11 (0.01)
<b>HAT</b>	<b>-0.02 (0.02)</b>	<b>-0.07 (0.02)</b>

Notice that the standard deviation of HAT is lower than the one reported by the big majority of the baselines (Table 1). This denotes a certain stability of HAT with respect to different task sequences, train/validation splits, and network initializations. Given the slightly increasing tendency of PNN with  $t$  (Fig. 3), one could contemplate the possibility that PNN would score above HAT for  $t > 8$ . However, we empirically found that that was not the case (presumably due to the capacity pre-assignment and parameter increase problems underlined in Sec. 3). In particular, we observed the gradual lowering of PathNet and PNN curves with increasing sequences of  $t \leq 8$  tasks, and also studied the case of  $t = 10$  tasks in the incremental class setting (see below and Appendix C.1).

## 4.2. Additional Results

Besides the motivated setup of the previous section, and in order to widen the strength of our results, we also run a number of experiments for other alternative setups. First, we consider an incremental class learning scenario, similar to Lopez-Paz & Ranzato (2017), using class subsets of both CIFAR10 and CIFAR100 data. In this setting, the best baseline after  $t \geq 3$  is EWC, with  $\rho^{\leq 10} = -0.18$ . HAT scores  $\rho^{\leq 10} = -0.12$  (33% forgetting reduction). Next, we consider the permuted MNIST sequence of tasks (Srivastava et al., 2013). In this setting, the best result we could find in the literature was from SI, with  $A^{\leq 10} = 97.1\%$ . HAT scores  $A^{\leq 10} = 98.5\%$  (48% error rate reduction). Finally, we also consider the 5-class MNIST task with 10 runs (Lee et al., 2017). In this setting, the best result from the literature corresponds to the conceptron-aided backpropagation approach (He & Jaeger, 2017), with  $A^{\leq 2} = 94.9\%$ . HAT scores  $A^{\leq 2} = 99.2\%$  (84% error rate reduction). The detail for all these results can be found in Appendix C.

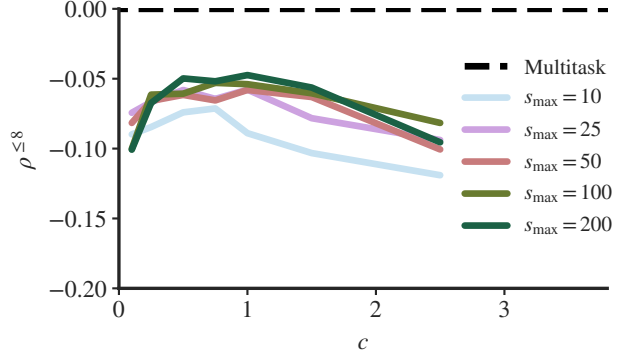


Figure 4. Effect of hyperparameters  $s_{\max}$  and  $c$  on average forgetting ratio  $\rho^{\leq 8}$ . Results for seed 0.

## 4.3. Hyperparameters

In any machine learning algorithm, it is important to assess the impact of its hyperparameters. HAT has two: the stability parameter  $s_{\max}$  and the compressibility parameter  $c$  (Secs. 2.4 and 2.6;  $s_{\max} \geq 1, c \geq 0$ ). A low  $s_{\max}$  provides plasticity to the units and capacity of adaptation, but the network may easily forget what it learned. A high  $s_{\max}$  prevents forgetting, but the network may have difficulties in adapting to new tasks. A low  $c$  allows to use almost all the network’s capacity for a given task, potentially spending too much in the current task. A high  $c$  forces it to learn a very compact model, at the expense of not reaching the accuracy that the original network could have reached. We empirically found good operation ranges  $s_{\max} \in [10, 200]$  and  $c \in [0.1, 2.5]$ . As we can see, any variation within these ranges results in reasonable performances (Fig. 4). Good parameter combinations were  $s_{\max} = 200$  and  $c = 0.5$ ,  $s_{\max} = 200$  and  $c = 1$ , or  $s_{\max} = 100$  and  $c = 0.75$ . Unless stated otherwise, we use the first combination in our experiments.

## 4.4. Monitoring and Network Pruning

It is interesting to note that the hard attention mechanism introduced in this paper offers a number of possibilities to monitor the behavior of our models. For instance, by computing the conditioning mask in Eq. 2 from the hard attention vectors  $\mathbf{a}_l^{\leq t}$ , we can assess which weights obtain a high attention value and compute an estimate of the instantaneous capacity usage (Fig. 5). Another facet we can monitor is the weight reuse across tasks. By a similar procedure, comparing the conditioning masks between tasks  $t_i$  and  $t_j$ ,  $j > i$ , we can assess the percentage of weights of task  $t_i$  that are reused in task  $t_j$  (Fig. 6).

A by-product of hard attention masks is that we can use them to assess which of the network’s weights are important, and then prune the most irrelevant ones (LeCun et al., 1990). This way, we can compress the network for further

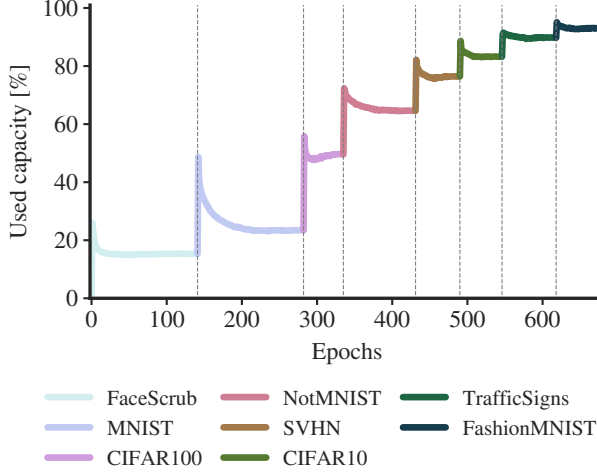


Figure 5. Network capacity usage with sequential task learning. Dashed vertical lines correspond to a task switch.

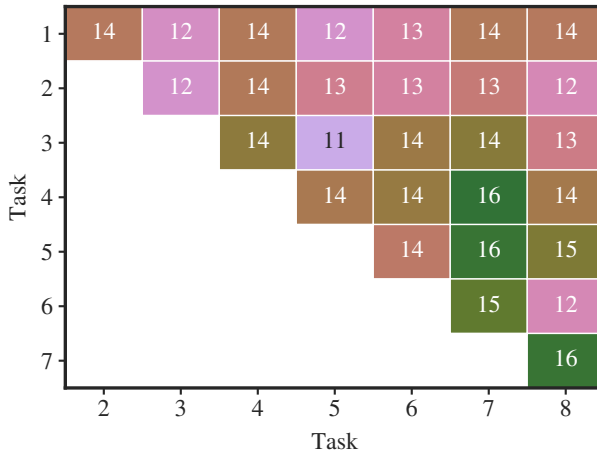


Figure 6. Percentage of weight reuse across tasks. Task sequence corresponds to: (1) FaceScrub, (2) MNIST, (3) CIFAR100, (4) NotMNIST, (5) SVHN, (6) CIFAR10, (7) TrafficSigns, and (8) FashionMNIST. Overlap across all 8 tasks was 0.4%.

deployment in low-resource devices or time-constrained environments (cf. Han et al., 2016). If we want to focus on such compression task, we can set  $c$  to a higher value than the one used for catastrophic forgetting and start with a positive random initialization of the embeddings  $\mathbf{e}_l$ . The former will promote more compression while the latter will ensure we start learning the model by putting attention to all weights in the first epochs (full capacity). We empirically found that using  $c = 1$  and  $\mathcal{U}(0, 2)$  yields a reasonable trade-off between accuracy and compression for the first task (Fig. 7). With that, we can compress the network to sizes between 26 and 2% of its original size, depending on the task (Appendix B.2). Comparing these numbers with the compression rates used by PackNet (50 or 25%), we see that HAT generally uses a much more compact model. Comparing with DEN on the specific MNIST and CIFAR100

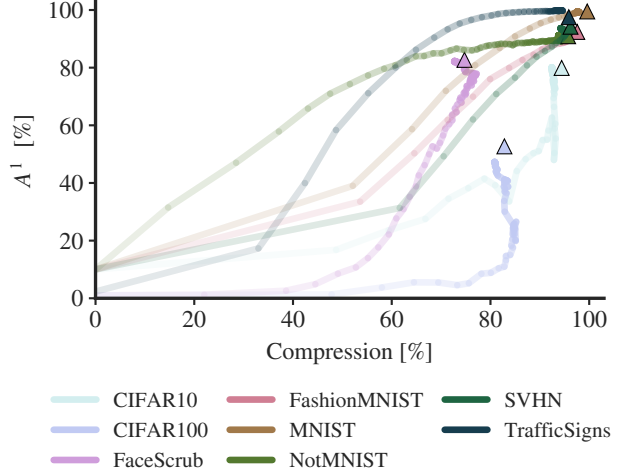


Figure 7. Data set accuracy  $A^1$  as a function of compression percentage. Every dot corresponds to an epoch and triangles correspond to the accuracy of the SGD approach (no compression).

tasks (18 and 52%), we find that HAT compresses to 2 and 19%, respectively. Interestingly, and in contrast to these and the majority of network pruning approaches, HAT learns the ranking used to prune network weights through SGD, and at the same time as the network weights themselves.

## 5. Conclusion

We introduce HAT, a hard attention mechanism that, by focusing on a task embedding, is able to protect the information of previous tasks while allowing the learning new tasks. This hard attention mechanism is lightweight, in the sense that it adds a minimum number of weights to the base network, and is trained together with the main model, with minimal overhead using vanilla SGD. We demonstrate the effectiveness of the approach to control catastrophic forgetting in the image classification context by running a series of experiments with multiple data sets and state-of-the-art approaches. HAT has only two hyperparameters which intuitively refer to the stability and compactness of the learned knowledge, and whose tuning we demonstrate is not crucial for obtaining good performance. In addition, HAT offers the possibility to monitor the used network capacity, the unit reuse across tasks, and the compressibility of a model trained for a given task. We hope that our approach may be also useful in online learning or network compression contexts, and that the hard attention mechanism presented here may find some applicability beyond the catastrophic forgetting problem.

## References

Anonymous. Memory-based parameter adaptation. *Int. Conf. on Learning Representations (ICLR)*, 2018.

Bakker, B. and Heskes, T. Task clustering and gating for bayesian multitask learning. *Journal of Machine Learning Research*, 4:83–99, 2003.

Bulatov, Y. NotMNIST dataset. Technical report, 2011. URL <http://yaroslavvb.blogspot.it/2011/09/notmnist-dataset.html>.

Clegg, B. A., DiGirolamo, G. J., and Keele, S. W. Sequence learning. *Trends in Cognitive Sciences*, 2(8):275–281, 1998.

Evgeniou, T. and Pontil, M. Regularized multi-task learning. In *Proc. of the ACM SIGKDD Int. Conf. on Knowledge Discovery and Data Mining (KDD)*, pp. 109–117, 2004.

Fernando, C., Banarse, D., Blundell, C., Zwols, Y., Ha, D., Rusu, A. A., Pritzel, A., and Wierstra, D. PathNet: evolution channels gradient descent in super neural networks. *ArXiv*, 1701.08734, 2017.

French, R. M. Using semi-distributed representations to overcome catastrophic forgetting in connectionist networks. In *Proc. of the Annual Conf. of the Cognitive Science Society (CogSci)*, pp. 173–178, 1991.

Glorot, X. and Bengio, Y. Understanding the difficulty of training deep feedforward neural networks. In *Proc. of the Int. Conf. on Artificial Intelligence and Statistics (AISTATS)*, pp. 249–256, 2010.

Goodfellow, I., Mizra, M., Da, X., Courville, A., and Bengio, Y. An empirical investigation of catastrophic forgetting in gradient-based neural networks. In *Proc. of the Int. Conf. on Learning Representations (ICLR)*, 2014.

Gutsein, S. and Stump, E. Reduction of catastrophic forgetting with transfer learning and ternary output codes. In *Proc. of the Int. Joint Conf. on Neural Networks (IJCNN)*, pp. 1–8, 2015.

Han, S., Mao, H., and Dally, W. J. Deep compression: compressing deep neural networks with pruning, trained quantization and Huffman coding. In *Proc. of the Int. Conf. on Learning Representations (ICLR)*, 2016.

He, X. and Jaeger, H. Overcoming catastrophic interference by conceptors. *ArXiv*, 1707.04853, 2017.

Jung, H., Ju, J., Jung, M., and Kim, J. Less-forgetting learning in deep neural networks. *ArXiv*, 1607.00122, 2016.

Kemelmacher-Shlizerman, I., Seitz, S. M., Miller, D., and Brossard, E. The megaface benchmark: 1 million faces for recognition at scale. In *Proc. of the IEEE Conf. on Computer Vision and Pattern Recognition (CVPR)*, pp. 4873–4882, 2016.

Kirkpatrick, J., Pascanu, R., Rabinowitz, N., Veness, J., Desjardins, G., Rusu, A. A., Milan, K., Quan, J., Ramalho, T., Grabska-Barwinska, A., Hassabis, D., Clopath, C., Kumaran, D., and Hadsell, R. Overcoming catastrophic forgetting in neural networks. *Proc. of the National Academy of Sciences of the USA*, 114(13):3521–3526, 2017.

Krizhevsky, A. Learning multiple layers of features from tiny images. Technical report, 2009. URL <https://www.cs.toronto.edu/~kriz/learning-features-2009-TR.pdf>.

Krizhevsky, A., Sutskever, I., and Hinton, G. ImageNet classification with deep convolutional neural networks. In Pereira, F., Burges, C. J. C., Bottou, L., and Weinberger, K. Q. (eds.), *Advances in Neural Information Processing Systems (NIPS)*, volume 25, pp. 1097–1105. 2012.

LeCun, Y., Denker, J. S., and Solla, S. A. Optimal brain damage. In Touretzky, D. S. (ed.), *Advances in Neural Information Processing Systems (NIPS)*, volume 2, pp. 598–605. Morgan Kaufmann, 1990.

LeCun, Y., Bottou, L., Bengio, Y., and Haffner, P. Gradient-based learning applied to document recognition. *Proceedings of the IEEE*, 86(11):2278–2324, 1998.

Lee, S.-W., Kim, J.-H., Jun, J., Ha, J.-W., and Zhang, B.-T. Overcoming catastrophic forgetting by incremental moment matching. In Guyon, I., Luxburg, U. V., Bengio, S., Wallach, H., Fergus, R., Vishwanathan, S., and Garnett, R. (eds.), *Advances in Neural Information Processing Systems (NIPS)*, volume 30, pp. 4655–4665. Curran Associates Inc., 2017.

Legg, S. and Hutter, M. Universal intelligence: a definition of machine intelligence. *Minds and Machines*, 17(4): 391–444, 2007.

Li, Z. and Hoiem, D. Learning without forgetting. *IEEE Trans. on Pattern Analysis and Machine Intelligence*, PP (99):1–1, 2017.

Lopez-Paz, D. and Ranzato, M. A. Gradient episodic memory for continuum learning. In Guyon, I., Luxburg, U. V., Bengio, S., Wallach, H., Fergus, R., Vishwanathan, S., and Garnett, R. (eds.), *Advances in Neural Information Processing Systems (NIPS)*, volume 30, pp. 6449–6458. Curran Associates Inc., 2017.

Mallya, A. and Lazebnik, S. PackNet: adding multiple tasks to a single network by iterative pruning. *ArXiv*, 1711.05769, 2017.

McCloskey, M. and Cohen, N. Catastrophic interference in connectionist networks: the sequential learning problem. *Psychology of Learning and Motivation*, 24:109–165, 1989.

Netzer, Y., Wang, T., Coates, A., Bissacco, A., Wu, B., and Ng, A. Reading digits in natural images with unsupervised feature learning. *NIPS Workshop on Deep Learning and Unsupervised Feature Learning*, 2011.

Ng, H.-W. and Winkler, S. A data-driven approach to cleaning large face datasets. In *Proc. of the IEEE Int. Conf. on Image Processing (ICIP)*, pp. 343–347, 2014.

Nguyen, C., Li, Y., Bui, T. D., and Turner, R. E. Variational continual learning. *ArXiv*, 1710.10628, 2017.

Ratcliff, R. Connectionist models of recognition memory: constraints imposed by learning and forgetting functions. *Psychological Review*, 97:285–308, 1990.

Rebuffi, S., Kolesnikov, A., Sperl, G., and Lampert, C. iCaRL: incremental classifier and representation learning. In *Proc. of the IEEE Conf. on Computer Vision and Pattern Recognition (CVPR)*, pp. 2001–2010, 2017.

Robins, A. Catastrophic forgetting, rehearsal and pseudorehearsal. *Connection Science*, 7:123–146, 1995.

Rusu, A. A., Rabinowitz, N. C., Desjardins, G., Soyer, H., Kirkpatrick, J., Kavukcuoglu, K., Pascanu, R., and Hadsell, R. Progressive neural networks. *ArXiv*, 1606.04671, 2016.

Shin, H., Lee, J. K., Kim, J., and Kim, J. Continual learning with deep generative replay. In Guyon, I., Luxburg, U. V., Bengio, S., Wallach, H., Fergus, R., Vishwanathan, S., and Garnett, R. (eds.), *Advances in Neural Information Processing Systems (NIPS)*, volume 30, pp. 2993–3002. Curran Associates Inc., 2017.

Srivastava, R. K., Masci, J., Kazerounian, S., Gomez, F., and Schmidhuber, J. Compete to compute. In Burges, C. J. C., Bottou, L., Welling, M., Ghahramani, Z., and Weinberger, K. (eds.), *Advances in Neural Information Processing Systems (NIPS)*, volume 26, pp. 2310–2318. Curran Associates Inc., 2013.

Stallkamp, J., Schlipsing, M., Salmen, J., and Igel, C. The German traffic sign recognition benchmark: a multi-class classification competition. In *Proc. of the Int. Joint Conf. on Neural Networks (IJCNN)*, pp. 1453–1460, 2011.

Thrun, S. and Mitchell, T. Lifelong robot learning. *Robotics and Autonomous Systems*, 15:25–46, 1995.

Venkatesan, R., Venkateswara, H., Panchanathan, S., and Li, B. A strategy for an uncompromising incremental learner. *ArXiv*, 1705.00744, 2017.

Xiao, H., Rasul, K., and Vollgraf, R. Fashion-MNIST: a novel image dataset for benchmarking machine learning algorithms. *ArXiv*, 1708.07747, 2017.

Yoon, J., Yang, E., Lee, J., and Hwang, S. J. Lifelong learning with dynamically expandable networks. *ArXiv*, 1708.0154, 2017.

Zenke, F., Poole, B., and Ganguli, S. Improved multitask learning through synaptic intelligence. In *Proc. of the Int. Conf. on Machine Learning (ICML)*, pp. 3987–3995, 2017.

## APPENDIX

### A. Data

The datasets we use in our experiments are summarized in Table 2. The MNIST dataset (LeCun et al., 1998) comprises  $28 \times 28$  monochromatic images of handwritten digits. Fashion-MNIST (Xiao et al., 2017) comprises gray-scale images of the same size from Zalando’s articles<sup>4</sup>. The German traffic sign dataset (TrafficSigns; Stallkamp et al., 2011) contains traffic sign images. We used the version of the dataset from the Udacity self-driving car github repository<sup>5</sup>. The NotMNIST dataset (Bulatov, 2011) comprises glyphs extracted from publicly available fonts, making a similar dataset to MNIST. We just need to resize the images<sup>6</sup>. The SVHN dataset (Netzer et al., 2011) comprises digits cropped from house numbers in Google Street View images. The FaceScrub dataset proposed by Ng & Winkler (2014) is widely used in face recognition tasks (Kemelmacher-Shlizerman et al., 2016). Because some of the images listed in the original dataset were not hosted anymore on the corresponding domains, we use a version of the data set stored on the MegaFace challenge website<sup>7</sup> (Kemelmacher-Shlizerman et al., 2016), from which we select the first 100 people with the most appearances<sup>8</sup>. The CIFAR10 and CIFAR100 datasets contain  $32 \times 32$  color images (Krizhevsky, 2009). To match the image input shape required in our experiments, some of the images in the corresponding datasets need to be resized (FaceScrub, TrafficSigns, and NotMNIST) or padded with zeros (MNIST and FashionMNIST). In addition, for the datasets comprising monochromatic images, we replicate the image across all RGB channels. We provide the necessary code to perform such adaptations in the corresponding links.

Table 2. Data sets used in the study: name, reference, number of classes, and number of train and test instances.

DATA SET	CLASSES	TRAIN	TEST
CIFAR10 (Krizhevsky, 2009)	10	50,000	10,000
CIFAR100 (Krizhevsky, 2009)	100	50,000	10,000
FACESCRUB (Ng & Winkler, 2014)	100	20,600	2,289
FASHIONMNIST (Xiao et al., 2017)	10	60,000	10,000
NOTMNIST (Bulatov, 2011)	10	16,853	1,873
MNIST (LeCun et al., 1998)	10	60,000	10,000
SVHN (Netzer et al., 2011)	100	73,257	26,032
TRAFFICSIGNS (Stallkamp et al., 2011)	43	39,209	12,630

### B. Raw Results

#### B.1. Task Mixture

We report all forgetting ratios  $\rho^{\leq t}$  for  $t = 1, \dots, 8$  in Table 3. A total of 10 runs with 10 different seeds are performed and the average and the standard deviation are taken.

#### B.2. Network Compression

The final results of the network compression experiments reported in the main paper (after reaching convergence) are available in Table 4. For the sake of comparison, we run HAT on isolated tasks and choose a different configuration with  $c = 1$ ,  $s_{\max} = 200$ , and uniform embedding initialization  $\mathcal{U}(0, 2)$ .

#### B.3. Training Time

To have an idea of the training time for each of the considered approaches, we report some reference values in Table 5. We see that HAT is also quite competitive in this aspect.

<sup>4</sup><https://github.com/zalandoresearch/fashion-mnist>

<sup>5</sup>[https://github.com/georgesung/traffic\\_sign\\_classification\\_german](https://github.com/georgesung/traffic_sign_classification_german)

<sup>6</sup>Code and data available on github: [https://github.com/nkundiushuti/notmnist\\_convert](https://github.com/nkundiushuti/notmnist_convert)

<sup>7</sup><http://megaface.cs.washington.edu/participate/challenge.html>

<sup>8</sup>Code and data available on github: [https://github.com/nkundiushuti/facescrub\\_subset](https://github.com/nkundiushuti/facescrub_subset)

Table 3. Average forgetting ratio  $\rho^{\leq t}$  for the considered approaches (10 runs, standard deviation into parenthesis).

APPROACH	$\rho^{\leq 1}$	$\rho^{\leq 2}$	$\rho^{\leq 3}$	$\rho^{\leq 4}$	$\rho^{\leq 5}$	$\rho^{\leq 6}$	$\rho^{\leq 7}$	$\rho^{\leq 8}$
LFL	-0.00 (0.01)	-0.73 (0.29)	-0.88 (0.18)	-0.89 (0.13)	-0.91 (0.11)	-0.90 (0.09)	-0.92 (0.08)	-0.92 (0.08)
LWF	-0.00 (0.01)	-0.14 (0.13)	-0.38 (0.17)	-0.63 (0.11)	-0.68 (0.08)	-0.70 (0.03)	-0.76 (0.06)	-0.80 (0.06)
SGD	-0.00 (0.00)	-0.20 (0.08)	-0.41 (0.09)	-0.49 (0.07)	-0.54 (0.07)	-0.57 (0.06)	-0.62 (0.06)	-0.66 (0.03)
IMM-MODE	-0.00 (0.01)	-0.11 (0.08)	-0.27 (0.12)	-0.37 (0.10)	-0.39 (0.07)	-0.45 (0.05)	-0.49 (0.06)	-0.49 (0.05)
SGD-F	-0.00 (0.00)	-0.20 (0.15)	-0.30 (0.15)	-0.38 (0.11)	-0.42 (0.09)	-0.44 (0.08)	-0.45 (0.07)	-0.44 (0.06)
IMM-MEAN	-0.00 (0.00)	-0.12 (0.10)	-0.24 (0.11)	-0.32 (0.06)	-0.37 (0.06)	-0.40 (0.06)	-0.42 (0.07)	-0.42 (0.04)
EWC	-0.00 (0.00)	-0.08 (0.06)	-0.15 (0.11)	-0.18 (0.07)	-0.21 (0.07)	-0.23 (0.04)	-0.25 (0.05)	-0.25 (0.03)
PATHNET	-0.02 (0.03)	-0.09 (0.16)	-0.11 (0.19)	-0.12 (0.21)	-0.14 (0.22)	-0.15 (0.23)	-0.17 (0.23)	-0.17 (0.23)
PNN	-0.10 (0.12)	-0.11 (0.10)	-0.13 (0.09)	-0.14 (0.04)	-0.13 (0.03)	-0.13 (0.02)	-0.12 (0.01)	-0.11 (0.01)
HAT	<b>-0.01 (0.01)</b>	<b>-0.02 (0.02)</b>	<b>-0.03 (0.03)</b>	<b>-0.04 (0.02)</b>	<b>-0.05 (0.03)</b>	<b>-0.06 (0.02)</b>	<b>-0.07 (0.03)</b>	<b>-0.07 (0.02)</b>

 Table 4. Results for the compression experiment reported in the main paper: accuracy  $A^1$  with SGD, accuracy  $A^1$  after compressing with HAT, and percentage of network weights used after compression.

DATA SET	RAW $A^1$	COMPRESSED $A^1$	SIZE [%]
CIFAR10	79.9%	80.0%	7.5%
CIFAR100	52.7%	47.3%	19.1%
FACESCRUB	82.7%	82.1%	27.1%
FASHIONMNIST	92.4%	92.3%	4.4%
MNIST	99.5%	99.4%	2.4%
NOTMNIST	90.9%	91.2%	6.2%
SVHN	94.2%	93.6%	5.7%
TRAFFICSIGNS	97.5%	98.9%	6.2%

## C. Additional Results

### C.1. Incremental CIFAR

As an additional experiment to complement our evaluation, we consider the incremental CIFAR setup, following a similar approach as [Lopez-Paz & Ranzato \(2017\)](#). We divide both CIFAR10 and CIFAR100 data sets into consecutive-class subsets and use them as tasks, presented in random order according to the seed. We take groups of 2 classes for CIFAR10 and 20 classes for CIFAR100, yielding a total of 10 tasks. We decide to take groups of 2 and 20 classes in order to have a similar number of training instances per task. The rest of the procedure is as in the main paper. The most important results are summarized there, and the complete numbers are depicted in Fig. 8 and reported in Table 6.

### C.2. Permuted MNIST

A common experiment is the one explained by [Srivastava et al. \(2013\)](#), and later employed to evaluate catastrophic forgetting by [Goodfellow et al. \(2014\)](#). It consists of taking random permutations of the pixels in the MNIST data set as tasks. Typically, the average accuracy after sequentially training on 10 MNIST permutations is reported. To match the different number of parameters used in the literature, we consider a small, medium, and a large networks based on a two-layer fully-connected architecture ([Zenke et al., 2017](#)) with 100, 500, and 2000 hidden units, respectively. For the large network we set dropout probabilities as [Kirkpatrick et al. \(2017\)](#). We use  $c = 1$  for the small network,  $c = 0.5$  for the medium and large networks, and  $s_{\max} = 200$ . The results are available in Table 7.

### C.3. Split MNIST

Another popular experiment is to split the MNIST data set into two tasks and report the average accuracy after learning them one after the other. In this case, the split is done with labels 0–4 and 5–9 ([Lee et al., 2017](#)), and the experiment is run for 10 times. We train HAT for 50 epochs and use  $c = 0.1$  and  $s_{\max} = 200$ . We match the base network architecture to the one used by [Lee et al. \(2017\)](#). Results are reported in Table 8.

Table 5. Training time measured on a single Titan X GPU: total, per epoch, and per batch (batches of 64). Batch processing time is measured for a forward pass (Batch-F), and for both a forward and a backward pass (Batch-FB).

APPROACH	TRAINING TIME			
	TOTAL [H]	EPOCH [S]	BATCH-F [MS]	BATCH-FB [MS]
PNN	6.0	4.1	10.2	27.5
PATHNET	4.5	3.6	10.6	23.9
EWC	3.9	3.1	7.9	19.7
IMM-MEAN	3.2	2.6	6.9	17.1
IMM-MODE	3.1	2.5	6.7	16.0
LWF	2.2	2.2	5.7	14.2
<b>HAT</b>	<b>2.2</b>	<b>1.6</b>	<b>4.0</b>	<b>11.7</b>
SGD	1.4	0.9	2.5	6.6
LFL	1.3	0.9	4.4	9.2
SGD-F	0.5	0.9	2.5	6.8

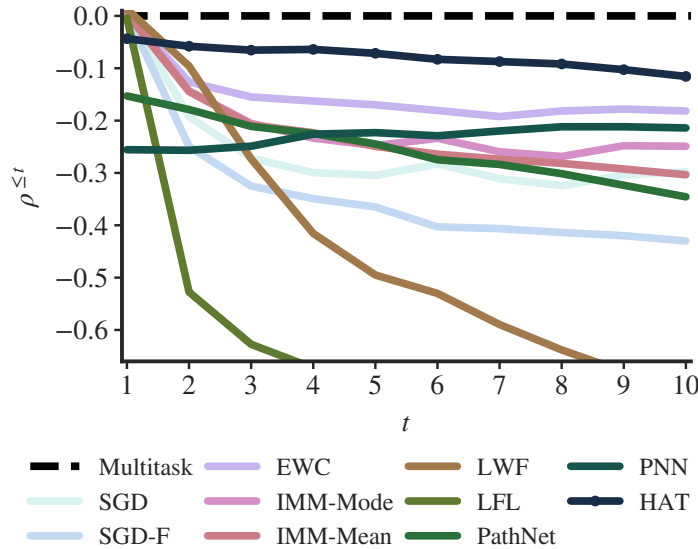


Figure 8. Average forgetting ratio  $\rho^{\leq t}$  for the incremental CIFAR task (10 runs).

Table 6. Average forgetting ratio  $\rho^{\leq t}$  for the incremental CIFAR task (10 runs, standard deviation into parenthesis).

APPROACH	$\rho^{\leq 1}$	$\rho^{\leq 2}$	$\rho^{\leq 3}$	$\rho^{\leq 4}$	$\rho^{\leq 5}$	$\rho^{\leq 6}$	$\rho^{\leq 7}$	$\rho^{\leq 8}$	$\rho^{\leq 9}$	$\rho^{\leq 10}$
LFL	-0.00 (0.01)	-0.53 (0.31)	-0.63 (0.25)	-0.67 (0.21)	-0.70 (0.20)	-0.74 (0.17)	-0.77 (0.15)	-0.79 (0.14)	-0.79 (0.14)	-0.78 (0.14)
LWF	-0.00 (0.02)	-0.10 (0.03)	-0.27 (0.05)	-0.42 (0.05)	-0.50 (0.06)	-0.53 (0.04)	-0.59 (0.06)	-0.64 (0.06)	-0.68 (0.05)	-0.70 (0.05)
SGD-F	-0.00 (0.01)	-0.25 (0.14)	-0.33 (0.16)	-0.35 (0.18)	-0.37 (0.16)	-0.40 (0.18)	-0.41 (0.18)	-0.41 (0.19)	-0.42 (0.19)	-0.43 (0.20)
PATHNET	-0.15 (0.31)	-0.18 (0.20)	-0.21 (0.26)	-0.22 (0.28)	-0.24 (0.29)	-0.27 (0.29)	-0.28 (0.30)	-0.30 (0.30)	-0.32 (0.29)	-0.35 (0.28)
SGD	-0.00 (0.01)	-0.19 (0.09)	-0.27 (0.09)	-0.30 (0.04)	-0.30 (0.06)	-0.28 (0.04)	-0.31 (0.03)	-0.32 (0.04)	-0.30 (0.05)	-0.30 (0.04)
IMM-MEAN	-0.00 (0.02)	-0.14 (0.08)	-0.21 (0.10)	-0.22 (0.10)	-0.25 (0.10)	-0.26 (0.08)	-0.27 (0.08)	-0.28 (0.08)	-0.29 (0.07)	-0.30 (0.07)
IMM-MODE	-0.00 (0.01)	-0.14 (0.10)	-0.21 (0.11)	-0.23 (0.06)	-0.25 (0.09)	-0.23 (0.07)	-0.26 (0.05)	-0.27 (0.04)	-0.25 (0.04)	-0.25 (0.04)
PNN	-0.26 (0.16)	-0.26 (0.08)	-0.25 (0.05)	-0.23 (0.04)	-0.22 (0.03)	-0.23 (0.03)	-0.22 (0.03)	-0.21 (0.02)	-0.21 (0.02)	-0.21 (0.02)
EWC	-0.00 (0.01)	-0.13 (0.09)	-0.15 (0.08)	-0.16 (0.07)	-0.17 (0.06)	-0.18 (0.06)	-0.19 (0.08)	-0.18 (0.07)	-0.18 (0.06)	-0.18 (0.06)
<b>HAT</b>	<b>-0.04 (0.03)</b>	<b>-0.06 (0.02)</b>	<b>-0.07 (0.01)</b>	<b>-0.06 (0.01)</b>	<b>-0.07 (0.01)</b>	<b>-0.08 (0.01)</b>	<b>-0.09 (0.01)</b>	<b>-0.09 (0.01)</b>	<b>-0.10 (0.01)</b>	<b>-0.12 (0.01)</b>

Table 7. Accuracy on the permuted MNIST task (Srivastava et al., 2013) taking the average after training 10 tasks. The only exception is the generative replay approach, whose performance was assessed after 5 tasks. Superscripts indicate results reported by (1) Nguyen et al. (2017) and (2) He & Jaeger (2017). An asterisk after parameter count indicates that the approach presents some additional structure not included in such parameter count (for instance, some memory module or an additional generative network).

APPROACH	PARAMETERS	$A^{\leq 10}$
GEM (LOPEZ-PAZ & RANZATO, 2017)	0.1 M*	82.8%
SI (ZENKE ET AL., 2017) <sup>1</sup>	0.1 M	86.0%
EWC (KIRKPATRICK ET AL., 2017) <sup>2</sup>	0.1 M	88.2%
MBPA + EWC – 1000 EX. (ANONYMOUS, 2018)	UNKNOWN*	89.7%
VCL (NGUYEN ET AL., 2017)	0.1 M*	90.0%
<b>HAT – SMALL</b>	<b>0.1 M</b>	<b>93.2%</b>
GENERATIVE REPLAY (SHIN ET AL., 2017)	UNKNOWN*	94.9%
CAB (HE & JAEGER, 2017)	0.7 M	95.2%
<b>HAT – MEDIUM</b>	<b>0.7 M</b>	<b>96.7%</b>
EWC (KIRKPATRICK ET AL., 2017)	5.8 M	96.9%
SI (ZENKE ET AL., 2017)	5.8 M	97.1%
<b>HAT – LARGE</b>	<b>5.8 M</b>	<b>98.5%</b>

Table 8. Average accuracy on the 5-class MNIST task (10 runs), following the setup of Lee et al. (2017) using 10 runs (standard deviation into parenthesis). Superscript (1) indicates results reported by Lee et al. (2017).

APPROACH	PARAMETERS	$A^{\leq 2}$
SGD (GOODFELLOW ET AL., 2014) <sup>1</sup>	1.9 M	71.3% (1.5)
L2-TRANSFER (EVGENIOU & PONTIL, 2004) <sup>1</sup>	1.9 M	85.8% (0.5)
IMM-MEAN (LEE ET AL., 2017)	1.9 M	94.0% (0.2)
IMM-MODE (LEE ET AL., 2017)	1.9 M	94.1% (0.3)
CAB (HE & JAEGER, 2017)	1.9 M	94.9% (0.3)
<b>HAT</b>	<b>1.9 M</b>	<b>99.2% (0.0)</b>